Proceeding of the IEEE
International Conference on Robotics and Biomimetics
Dali, China, December 2019

Task Cartesian Coordinate Frame based High Precision 3-D Adaptive Robust Contouring Control

Zhihao Zhang, Ran Shi, *Student Member, IEEE*, Yunjiang Lou, *Senior Member, IEEE*

***Abstract*— Contouring error is an important index for the surface precision of work pieces in tracking motion. In this paper, for settle the contouring error estimation which is only calculated on tangent line along the desired trajectory and improve 3-D contouring performance under disturbances, an adaptive robust controller (ARC) is adopted in task cartesian coordinate frame (TCCF). In addition, The TCCF can reduce the number of controller from three dimension regulation problem to two which is compared with the task coordinate frame (TCF). Theoretically, the controller is proved that the stability can be achieved. Experiments are conducted in a three-axis servo system. Compared with computed-torque controller (CTC), ARC in TCCF can get higher overall contouring precision under the disturbances drastically and reduce the number of controllers.**

I. INTRODUCTION

In traditional machine tool control, typically a three axis motion control platform, which is controlled as decoupled single axis structure. If one axis is affected by disturbance, however, the other axes move as usual, the contouring performance will degrade for uncoordination [1].

Contouring error is a shortest distance from the actual location to the desired curve [2] . In the typical trajectory tracking tasks, such as laser cutting, grinding and painting, contouring error control decide the precision of final work pieces [3]. Thus, It's very important to control contouring error coordinately and directly.

Commonly, there are two main contouring control methods. The first is based on cross-coupled control (CCC) [2]. In this, the contouring error is compensated to each motion axis. However, it is difficult to calculate the control gains when in 3-D contouring [4]. The second is based on coordinate transformation that the system dynamics is transformed to a suitable coordinate frame. The contouring error dynamics can be expressed and controlled directly. There are some type of coordinate frames were raised in literatures, such as task cartesian frame (TCF) [5], task polar coordinate frame (TPCF) [6], and global TCF (GTCF) [4]. In TCF, contouring error is estimated as the distance from the actual location to the tangent line which is attached to tracked point at desired trajectory. Thus, the accuracy of estimated contouring error will decline at much larger curvature trajectory. Compared with TCF, TPCF improves contouring accuracy at the large curvature curve since it is established by the local osculating circle. However, above these two methods are based local characteristics of desired curve. In GTCF, the estimated contouring error is the first-order approximation of desired curve exactly. In addition, Yao and Hu [7]–[9] have been used a adaptive robust controller to suppress the system model parameter uncertainties and external disturbances mightily by designing a large size adaptive parameter matrix function. Although the latter two methods can get high contouring performance, they are only suitable for 2-D trajectory.

In order to improve the performance in 3-D contouring control, Shi [3] proposed a novel TCF (Task Cartesin Coordinate Frame, TCCF). The establishment of TCCF is independed on specified contouring error estimation method which means some high precision estimated methods can be used in TCCF. Beside this, in TCCF, the system dynamic model will be transformed to a two dimension decoupled error control problem in the advancing and contouring direction, respectively. However, this method did not explicitly address the effect of invariable system dynamic parameters and external disturbances.

In this paper, for the purpose of improving the 3-D contouring performance under system dynamic parameters uncertainties and externally disturbances, the ARC is developed in TCCF. In section II, the TCCF will be introduced briefly and the system dynamics in TCCF will be derived. In section III, the briefly theoretical proof of ARC and the detailed design process in TCCF is given. Experiments are demonstrated for three-dimensional contours and contouring index are discussed and compared in section IV. Conclusion is given in section V.

II. PROBLEM FORMULATION

A. Task Cartesian Coordinate Frame (TCCF)

The contouring error vector is decomposed three parts which is controlled respectively on the each coordinate axis in TCF. For using arbitrary general contour approximate, e.g., circular approximation [6], canonical expansion estimation [10] or Newton-Based method [11], estimating the contouring error position E and control error directly, the TCF is transformed from the desired position D to the estimated contouring error position E. Using E, A and the current desired position D, as shown in Fig. 1, TCCF can be setup by these following procedures.

1) Set E as the origin of TCCF.

Zhang, Shi and Lou (the corresponding author) are with the School of Mechatronics Engineering and Automation, Harbin Institute of Technology (Shenzhen), Shenzhen, China zhangzhihao@stu.hit.edu.cn (zhang); hit.shi.ran@gmail.com (Shi); louyj@hitsz.edu.cn (Lou)

This work was supported partially by the NSFC-Shenzhen Robotics Basic Research CenterProgram (No. U1713202) and partially by the Shenzhen Science and Technology Program (No.JCYJ20180508152226630).

978-1-7281-6321-5/19//$31.00 ©2019 IEEE

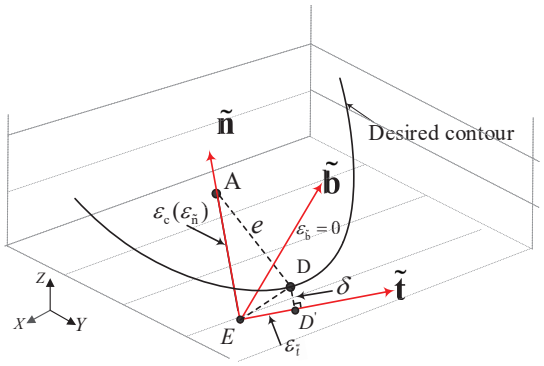

Fig. 1. The Task Cartesian Coordinate Frame

2) The unit vector of $\overrightarrow{EA}$ is named as $\tilde{\mathbf{n}}$. It's unit vector $\tilde{\mathbf{n}}$ computed by

$$\tilde{\mathbf{n}} = \frac{\overrightarrow{EA}}{||\overrightarrow{EA}||} \tag{1}$$

3) Another axis in TCCF is named $\tilde{\mathbf{b}}$ which is vertical to the plane constructed by position A, E, D. It can be calculated by

$$\tilde{\mathbf{b}} = \frac{\overrightarrow{ED} \times \overrightarrow{EA}}{||\overrightarrow{ED} \times \overrightarrow{EA}||} \tag{2}$$

4) The third axis in TCCF is named $\tilde{\mathbf{t}}$ which is calculated by the right-hand rule. So the $\tilde{\mathbf{t}}$ axis can be calculated as

$$\tilde{\mathbf{t}} = \tilde{\mathbf{n}} \times \tilde{\mathbf{b}} \tag{3}$$

Since when $\overrightarrow{EA} = 0$ or $\overrightarrow{ED} \times \overrightarrow{EA} = 0$, equations (1) and (2) are not be established and we can not set up TCCF by these procedures. This case means that A and E, or E and D, or all locate on a line or point. In this case, We will replace TCCF with TCF at E by coordinate transformation.

B. Contouring Error in TCCF

Firstly, the transformation equation which is between TCCF and the world Cartesian coordinate frame (WCCF) each other is shown as

$$T_{tw} : \mathbf{p} = \mathbf{R}\mathbf{p_t} + \mathbf{p_e} \tag{4}$$

$$T_{wt} : \mathbf{p_t} = \mathbf{R}^{-1}(\mathbf{p} - \mathbf{p_e}) \tag{5}$$

In TCCF, the $\mathbf{R}$ is a coordinate transformation matrix from TCCF to WCCF, $\mathbf{R} = [\tilde{\mathbf{t}} \quad \tilde{\mathbf{n}} \quad \tilde{\mathbf{b}}]$. The $\mathbf{R}$ is a unitary matrix, i.e., $\mathbf{R}^{-1} = \mathbf{R}^{\mathrm{T}}$. In addition, $\mathbf{R}$ is a time-varying transformation matrix along the desired trajectories. $\mathbf{p_t}$ and $\mathbf{p}$ represent the same coordinate in TCCF and WCCF, respectively. $\mathbf{p_e}$ is the estimated contouring error position E in WCCF. From (4) and (5), error vector $\mathbf{e}$ in WCCF can be transformed to the tracking error vector ε in TCCF.

$\mathbf{p} = [x(t), y(t), z(t)]^{\mathrm{T}}$ and $\mathbf{p_d} = [x_d(t), y_d(t), z_d(t)]^{\mathrm{T}}$ are respectively coordinate position of A and D in WCCF. $\mathbf{p_t} = [\tilde{t}_A \quad \tilde{n}_A \quad \tilde{b}_A]^{\mathrm{T}}$ and $\mathbf{p_{dt}} = [\tilde{t}_D \quad \tilde{n}_D \quad \tilde{b}_D]^{\mathrm{T}}$ are the coordinate vector of A and D in TCCF. From equation (5), $\mathbf{e} = \mathbf{p} - \mathbf{p_d}$ in TCCF can be written as

$$\begin{aligned} \varepsilon = \mathbf{p_t} - \mathbf{p_{dt}} &= \begin{bmatrix} \tilde{t}_A - \tilde{t}_D \\ \tilde{n}_A - \tilde{n}_D \\ \tilde{b}_A - \tilde{b}_D \end{bmatrix} \\ &= \mathbf{R}^{\mathrm{T}}(\mathbf{p} - \mathbf{p_e}) - \mathbf{R}^{\mathrm{T}}(\mathbf{p_d} - \mathbf{p_e}) = \mathbf{R}^{\mathrm{T}}\mathbf{e} \end{aligned} \tag{6}$$

From Fig.1, the third coordinate component of $\tilde{\mathbf{b}}$ is zero with A and D at one coordinate plane, i.e., $\tilde{b}_A = \tilde{b}_D = 0$ and $\tilde{t}_A = 0$. Therefore, the contouring error in (6) is rewritten

$$\varepsilon = \begin{bmatrix} \varepsilon_{\tilde{t}} \\ \varepsilon_{\tilde{n}} \\ 0 \end{bmatrix} - \begin{bmatrix} 0 \\ \tilde{n}_D \\ 0 \end{bmatrix} = \hat{\varepsilon} - \delta, \tag{7}$$

From this equation show, the tracking error vector ε is decomposed into three parts where $\varepsilon_{\tilde{t}} = \tilde{t}_A - \tilde{t}_D = -\tilde{t}_D$ is named advancing direction error and $\varepsilon_{\tilde{n}} = \tilde{n}_A$ is contouring error, the third component is zero. The $\hat{\varepsilon} = [\varepsilon_{\tilde{t}} \quad \varepsilon_{\tilde{n}} \quad \varepsilon_{\tilde{b}}]^{\mathrm{T}}$ is controlled value in TCCF which equals ε plus δ and $\varepsilon_{\tilde{b}} = 0$. Since the contouring error is indicated in the $\tilde{\mathbf{t}}\tilde{\mathbf{n}}$ plane, it's third element must equal zero.

In this way, not only the appropriate contouring error calculation method can be selected according to the precision requirements and computing speed of the system, but also the 3-D regulation problem can be converted into a 2-D control problem.

C. System Dynamics

System dynamic of three axis motion platform can be written as

$$\mathbf{M}\ddot{\mathbf{p}} + \mathbf{B}\dot{\mathbf{p}} + \mathbf{F}(\dot{\mathbf{p}}) = \mathbf{u_t} + \mathbf{d}, \tag{8}$$

where $\mathbf{p}$, $\dot{\mathbf{p}}$, $\ddot{\mathbf{p}}$ are position, velocity and acceleration vectors, respectively in task space; $\mathbf{u_t}$ is control input, $\mathbf{d}$ is the 3×1 vector of unknown external disturbances; $\mathbf{M} = \mathrm{diag}[M_1, M_2, M_3]$ and $\mathbf{B} = \mathrm{diag}[B_1, B_2, B_3]$ are the 3×3 diagonal mass and damping matrices, respectively;$\mathbf{F}(\dot{\mathbf{p}}) = [F_1(\dot{x}), F_2(\dot{y}), F_3(\dot{z})]^{\mathrm{T}}$ is a external coulomb friction disturbance and $\mathbf{F}(\dot{\mathbf{p}}) = \mathbf{A}\mathbf{f}(\dot{\mathbf{p}})$, where $\mathbf{A} = \mathrm{diag}[A_1, A_2, A_3]$ is 3×3 diagonal friction amplitude and $\mathbf{f}(\cdot)$ is a continuous tangent function [12], i.e., $\mathbf{f}(\dot{\mathbf{p}}) = [f(\dot{x}), f(\dot{y}), f(\dot{z})]^{\mathrm{T}}$. Then, from the (8) , we can get the error dynamic function

$$\mathbf{M}\ddot{\mathbf{e}} + \mathbf{B}\dot{\mathbf{e}} + \mathbf{A}\mathbf{f}(\dot{\mathbf{p}}) + \mathbf{M}\ddot{\mathbf{p}}_\mathbf{d} + \mathbf{B}\dot{\mathbf{p}}_\mathbf{d} = \mathbf{u} + \mathbf{d_n} + \tilde{\mathbf{d}} \tag{9}$$

where $\mathbf{d_n} = [d_{n1}, d_{n2}, d_{n3}]^T$ is the nominal value of lumped modeling error, $\tilde{\mathbf{d}}$ is uncertain nonlinearities part.

By (7), the time derivatives of the tracking error states can be written as

$$\dot{\mathbf{e}} = \mathbf{R}\dot{\varepsilon} + \dot{\mathbf{R}}\varepsilon \qquad \ddot{\mathbf{e}} = \mathbf{R}\ddot{\varepsilon} + 2\dot{\mathbf{R}}\dot{\varepsilon} + \ddot{\mathbf{R}}\varepsilon \tag{10}$$

Then the dynamic system can be rewritten in TCCF and multiply an $\mathbf{R}^{\mathrm{T}}$ on both sides, then

$$\begin{aligned} \mathbf{M_t}\ddot{\varepsilon} + \mathbf{B_t}\dot{\varepsilon} + 2\mathbf{C_t}\dot{\varepsilon} + \mathbf{D_t}\varepsilon + \mathbf{M_p}\ddot{\mathbf{p}}_\mathbf{d} + \mathbf{B_p}\dot{\mathbf{p}}_\mathbf{d} + \mathbf{A_p}\mathbf{f}(\dot{\mathbf{p}}) \\ = \mathbf{u_t} + \mathbf{d_t} + \tilde{\Delta} \end{aligned} \tag{11}$$

where

$$\mathbf{M_t} = \mathbf{R}^{\mathrm{T}}\mathbf{M}\mathbf{R},\ \mathbf{B_t} = \mathbf{R}^{\mathrm{T}}\mathbf{B}\mathbf{R},\ \mathbf{C_t} = \mathbf{R}^{\mathrm{T}}\mathbf{M}\dot{\mathbf{R}}$$
$$\mathbf{D_t} = \mathbf{R}^{\mathrm{T}}(\mathbf{M}\ddot{\mathbf{R}} + \mathbf{B}\dot{\mathbf{R}}),\ \mathbf{u_t} = \mathbf{R}^{\mathrm{T}}\mathbf{u},\ \mathbf{d_t} = \mathbf{R}^{\mathrm{T}}\mathbf{d_n},\ \tilde{\Delta} = \mathbf{R}^{\mathrm{T}}\tilde{\mathbf{d}}$$
$$\mathbf{M_p} = \mathbf{R}^{\mathrm{T}}\mathbf{M},\ \mathbf{B_p} = \mathbf{R}^{\mathrm{T}}\mathbf{B},\ \mathbf{A_p} = \mathbf{R}^{\mathrm{T}}\mathbf{A} \tag{12}$$

However, for control the advancing error and contouring error directly in TCCF, the ε of system dynamics should be converted to $\hat{\varepsilon}$. Based on (7), then the (11) can be written as

$$\mathbf{M_t}\ddot{\hat{\varepsilon}} + \mathbf{B_t}\dot{\hat{\varepsilon}} + 2\mathbf{C_t}\dot{\hat{\varepsilon}} + \mathbf{D_t}\hat{\varepsilon} + \mathbf{M_p}\ddot{\mathbf{p}}_\mathbf{d} + \mathbf{B_p}\dot{\mathbf{p}}_\mathbf{d} + \mathbf{A_p}\mathbf{f}(\dot{\mathbf{p}}) = \mathbf{u_t} + \mathbf{u_d} + \mathbf{d_t} + \tilde{\Delta} \tag{13}$$

where $\mathbf{u_d} = \mathbf{M_t}\ddot{\delta} + \mathbf{B_t}\dot{\delta} + 2\mathbf{C_t}\dot{\delta} + \mathbf{D_t}\delta$.

There are three properties of (13) [9].

(A1) $\mathbf{M_t}$ is a symmetric positive-definite (s.p.d) matrix in a finite manipulating space $\mathbf{p} \in \Omega_\mathbf{p}$

$$u_1\mathbf{I} \leqslant \mathbf{M_t} \leqslant u_2\mathbf{I} \qquad \forall \mathbf{p} \in \Omega_\mathbf{p} \tag{14}$$

u_1 and u_2 are two positive scalars and $\mathbf{I}$ is 3×3 unit diagonal matrix.

(A2) Given the definitions in (12), the matrix $\mathbf{N} = \dot{\mathbf{M}}_\mathbf{t} - 2\mathbf{C_t}$ is a skew-symmetric matrix.

(A3) $\theta = [\theta_1, \ldots, \theta_{12}]^{\mathrm{T}} = [M_1, M_2, M_3, B_1, B_2, B_3, A_1, A_2, A_3, \quad d_{n1}, d_{n2}, d_{n3}]^{\mathrm{T}}$ is a parameter vector of $\mathbf{M_t}$, $\mathbf{B_t}$, $\mathbf{C_t}$, $\mathbf{D_t}$, $\mathbf{M_p}$, $\mathbf{B_p}$, $\mathbf{A_p}$ and $\mathbf{d_t}$ in (13).

Actually, the parameter vector θ can be predicted in a limited range. The range of θ are known, i.e.,

$$\theta \in \Omega_\theta \triangleq \{\theta : \theta_{min} \leqslant \theta \leqslant \theta_{max}\} \tag{15}$$
$$\tilde{\Delta} \in \Omega_\Delta \triangleq \{\tilde{\Delta} : ||\tilde{\Delta}|| \leqslant \delta_\Delta\} \tag{16}$$

where $\theta_{min} = [\theta_{1min}, \cdots, \theta_{12min}]^{\mathrm{T}}$ and $\theta_{max} = [\theta_{1max}, \cdots, \theta_{12max}]^{\mathrm{T}}$ and δ_Δ can be predicted, .

III. Adaptive Robust Controller Design

A. ARC Law Design

In this section, the ARC design based on TCCF will be introduced. Specially, a sliding-mode function is

$$\mathbf{s} = \dot{\hat{\varepsilon}} + \Lambda\hat{\varepsilon} \tag{17}$$

Where $\mathbf{s}$ is a proportional-differential (PD) feedback of contouring error. $\Lambda > 0$ is a positive diagonal proportion matrix.

Because the third element of $\hat{\varepsilon}$ is always zero, the third of vector $\mathbf{s}$ is zero too. Essentially, define a Lyapunov function

$$V(t) = \frac{1}{2}\mathbf{s}^{\mathrm{T}}\mathbf{M_t}\mathbf{s} \tag{18}$$

Differential of V is

$$\dot{V} = \mathbf{s}^{\mathrm{T}}\mathbf{M_t}\dot{\mathbf{s}} + \frac{1}{2}\mathbf{s}^{\mathrm{T}}\dot{\mathbf{M}}_\mathbf{t}\mathbf{s} \tag{19}$$

where according to (A2), the term $(1/2)\mathbf{s}^{\mathrm{T}}\dot{\mathbf{M}}_\mathbf{t}\mathbf{s} = \mathbf{s}^{\mathrm{T}}\mathbf{C_t}\mathbf{s}$ and take (13), (17) into (19), then can get

$$\dot{V} = \mathbf{s}^{\mathrm{T}}[\mathbf{u_t} + \mathbf{d_t} + \mathbf{u_d} + \tilde{\Delta} - \mathbf{M_p}\ddot{\mathbf{p}}_\mathbf{d} - \mathbf{B_p}\dot{\mathbf{p}}_\mathbf{d} - \mathbf{A_p}\mathbf{S_f}(\dot{\mathbf{p}}) - \mathbf{B_t}\dot{\hat{\varepsilon}} - \mathbf{C_t}\dot{\hat{\varepsilon}} - \mathbf{D_t}\hat{\varepsilon} + \mathbf{C_t}\Lambda\hat{\varepsilon} + \mathbf{M_t}\Lambda\dot{\hat{\varepsilon}}] \tag{20}$$

From (A3) and (20), we can rewrite the terms in (20) as

$$\mathbf{M_p}\ddot{\mathbf{p}}_\mathbf{d} + \mathbf{B_p}\dot{\mathbf{p}}_\mathbf{d} + \mathbf{A_p}\mathbf{f}(\dot{\mathbf{p}}) + \mathbf{B_t}\dot{\hat{\varepsilon}} + \mathbf{C_t}\dot{\hat{\varepsilon}} + \mathbf{D_t}\hat{\varepsilon} - \mathbf{C_t}\Lambda\hat{\varepsilon} - \mathbf{M_t}\Lambda\dot{\hat{\varepsilon}} - \mathbf{d_t} - \mathbf{u_d} = -\mathbf{W}(\mathbf{p}, \dot{\mathbf{p}}, \mathbf{p_d}, t)\theta \tag{21}$$

where $\mathbf{W}(\mathbf{p}, \dot{\mathbf{p}}, \mathbf{p_d}, t)$ is a 3×12 matrix function. It can be got by expanding the left-side term of (21) and taking the each content of θ as an independent variable, the coefficients of θ are the contents of $\mathbf{W}$. The (20) can be rewritten as

$$\dot{V} = \mathbf{s}^{\mathrm{T}}[\mathbf{u_t} + \mathbf{W}(\mathbf{p}, \dot{\mathbf{p}}, \mathbf{p_d}, t)\theta + \tilde{\Delta}] \tag{22}$$

The structure of controller is:

$$\mathbf{u_t} = \mathbf{u_a} + \mathbf{u_s} \qquad \mathbf{u_a} = -\mathbf{W}(\mathbf{p}, \dot{\mathbf{p}}, \mathbf{p_d}, t)\hat{\theta} \tag{23}$$

Where $\mathbf{u_a}$ is an adaptive controller, which is used to adjust the system parametric θ in a range dynamically and adaptively with system affected by environment; $\mathbf{u_r}$ is robust controller, which is used to eliminate system unknown disturbance and system asymptotic output stable guaranteed under parametric uncertainties only; $\hat{\theta}$ is estimated value by $\mathbf{u_a}$. Substituting (23) to (22) and the result is

$$\dot{V} = \mathbf{s}^{\mathrm{T}}[\mathbf{u_r} - \mathbf{W}(\mathbf{p}, \dot{\mathbf{p}}, \mathbf{p_d}, t)\tilde{\theta} + \tilde{\Delta}] \tag{24}$$

where the $\tilde{\theta} = \hat{\theta} - \theta$ is estimated error of θ. The robust controller $\mathbf{u_r}$ is consisted by two parts:

$$\mathbf{u_r} = \mathbf{u_{r1}} + \mathbf{u_{r2}} \qquad \mathbf{u_{r1}} = -\mathbf{K}\mathbf{s} \tag{25}$$

where $\mathbf{u_{r1}}$ is utilized to stabilize the controlled system, and $\mathbf{K}$ is a positive gain diagonal matrix with the $\mathbf{s}$, and $\mathbf{u_{r2}}$ is a feedback used to suppress the model uncertainties. For satisfying the system model uncertainties attenuated, the $\mathbf{u_{r2}}$ need to following the two conditions [8]:

$$1)\quad \mathbf{s}^{\mathrm{T}}\{\mathbf{u_{r2}} - \mathbf{W}(\mathbf{p}, \dot{\mathbf{p}}, \mathbf{p_d}, t)\tilde{\theta} + \tilde{\Delta}\} \leqslant \eta$$
$$2)\quad \mathbf{s}^{\mathrm{T}}\mathbf{u_{r2}} \leqslant 0 \tag{26}$$

where η is a arbitrary small parameter. If $\mathbf{u_{r2}} = -\mathbf{K_2}\mathbf{s}$, where $\mathbf{K_2}$ is a large enough positive diagonal matrix, the two conditions must be satisfied.

In TCCF, current actual point $\mathbf{p}$ and desired point $\mathbf{p_d}$ are located on the $\tilde{\mathbf{t}}\tilde{\mathbf{n}}$ plane, so the elements in third row of matrix function $\mathbf{W}(\mathbf{p}, \dot{\mathbf{p}}, \mathbf{p_d}, \mathbf{t})$ must be zero. Moreover, since the third element of the vector $\mathbf{s}$ is zero, the third control value of robust controller $\mathbf{u_s}$ also must be zero. That means there are only two controllers needed to tune in adaptive robust controller which archive take 3-D regulation problem to 2-D.

B. Adaptive Law and Controller Stability Prove

This section will introduce the adaptive update law of $\hat{\theta}$. The parameter adaptive update law can be written as:

$$\dot{\hat{\theta}} = -\Gamma\Upsilon \tag{27}$$

In order to guarantee $\dot{\hat{\theta}}$ in the setting range, we should update the $\hat{\theta}$ according to actual situation of the system.

The adaptive law can be written like

$$\dot{\hat{\theta}}_i = \begin{cases} 0, & \text{if } \hat{\theta}_i \geqslant \theta_{imax} \text{ and } \dot{\hat{\theta}}_i > 0, \\ 0, & \text{if } \hat{\theta}_i \leqslant \theta_{imin} \text{ and } \dot{\hat{\theta}}_i < 0, \\ \dot{\hat{\theta}}_i, & \text{otherwise.} \end{cases} \tag{28}$$

This adaptive parameter update law is named discontinuous projection adaptive update law [8]. Υ is an adaption function, (28) guarantees the following properties:

$$\hat{\theta} \in \Omega_\theta \triangleq \{\hat{\theta} : \theta_{min} \leqslant \hat{\theta} \leqslant \theta_{max}\} \tag{29}$$

$$\tilde{\theta}^T(\Gamma^{-1}\dot{\hat{\theta}} - \Upsilon) \leqslant 0 \tag{30}$$

In (27),the adaption function is written as

$$\Upsilon = \mathbf{W^T}(\mathbf{p}, \dot{\mathbf{p}}, \mathbf{p_d}, t)\mathbf{s}. \tag{31}$$

Finally, there will give the proof of ARC control law stability.

1) Since the actual control system is bounded, the $V(t)$ defined by (26) has been limited like

$$V(t) \leqslant e^{(-\alpha t)}V(0) + \frac{\eta}{\alpha}[1 - e^{(-\alpha t)}] \tag{32}$$

where $\alpha = 2\sigma_{min}(K)/u_2$ and σ_{min} is a function which denotes the minimum eigenvalue of a matrix.

From (14), there can get

$$\frac{1}{2}u_1||\mathbf{s}||^2 \leqslant V(t) \leqslant \frac{1}{2}u_2||\mathbf{s}||^2 \tag{33}$$

From (22), (25), 1) of (26) and (33). Thus, then

$$\begin{aligned} \dot{V}(t) &= -\mathbf{s^T}\mathbf{K}\mathbf{s} + \mathbf{s^T}[\mathbf{u_{s2}} - \mathbf{W}(\mathbf{p}, \dot{\mathbf{p}}, \mathbf{p_d}, t)\tilde{\theta} + \tilde{\Delta}] && (34) \\ &\leqslant -\sigma_{min}(K)||\mathbf{s}||^2 + \eta && (35) \\ &= -\alpha V + \eta \end{aligned}$$

Then (32) can be got by this result.

2) If there are only uncertainties of parameter during finite time t_0, i.e., $\tilde{\Delta} = 0\ \forall t \geqslant t_0$. Then, expect the result of 1), the tracking error will be zero, i.e., $\mathbf{e} \to 0$ and $\mathbf{s} \to 0$ as $t \to \infty$.

Now consider the situation that $\tilde{\Delta} = 0$, $\forall t \leqslant t_0$. The p.d function $V_\theta(t)$ is chosen as

$$V_\theta(t) = V(t) + \frac{1}{2}\tilde{\theta}^T\Gamma^{-1}\tilde{\theta} \tag{36}$$

Nothing(34), 2) of (26) and (30), then

$$\begin{aligned} \dot{V}_\theta(t) &\leqslant -\mathbf{s^T}\mathbf{K}\mathbf{s} - \mathbf{s^T}\mathbf{W}(\mathbf{p}, \dot{\mathbf{p}}, \mathbf{p_d}, t)\tilde{\theta} + \tilde{\theta}^T\Gamma^{-1}\dot{\hat{\theta}} && (37) \\ &= -\mathbf{s^T}\mathbf{K}\mathbf{s} + \tilde{\theta}^T[\Gamma^{-1}\dot{\hat{\theta}} - \mathbf{W^T}(\mathbf{p}, \dot{\mathbf{p}}, \mathbf{p_d}, t)\mathbf{s}] && (38) \\ &\leqslant -\mathbf{s^T}\mathbf{K}\mathbf{s} \end{aligned}$$

Therefore, $\mathbf{s}$ is square-integral. And the $\dot{\mathbf{s}}$ is bounded which can be known. So, from the Barbalat's lemma, $\mathbf{s} \to 0$ and $\mathbf{e} \to 0$ as $t \to \infty$.

This also explains the reason that controller asymptotically output tracking under dynamic parametric uncertainties only. However, the actual system always exists uncontrollable disturbances, thus, the tracking error can't reach zero.

IV. Experiment And Discussion

A. Experimental Setup

For verifying the proposed controller's performance applied in contouring-error control, a three-axis motion platform is used. The precision of encoder is 0.5 μm. In Fig. 2, the servo motors and the drivers are respectively MSMD012P1C and MADDT1205 both from Panasonic. The dSPACE MicroLabBox is used as real time controller. And a PC is used to send and receive motion instruction and position feedback through the controller at 1KHz. The proposed and comparative control approaches are programmed in MATLAB/Simulink in Windows 7 environment.

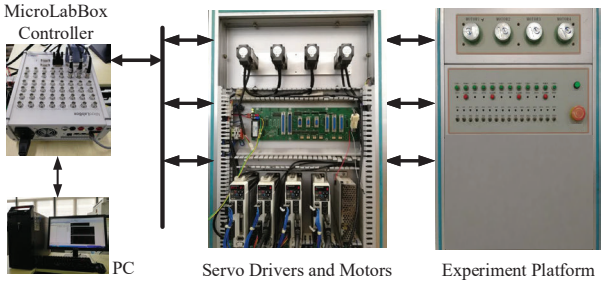

Fig. 2. Experimental Setup

B. Evaluation Indexes

The root mean square (RMS) value of the contouring error, $\varepsilon_r = (\frac{1}{T}\int_0^T |\varepsilon_c| d_t)^{\frac{1}{2}}$.

The max value of the contouring error absolute value, $\varepsilon_m = \max\{|\varepsilon_c|\}$.

The root mean square (RMS) value of the tracking error, $e_r = (\frac{1}{T}\int_0^T |e| d_t)^{\frac{1}{2}}$.

The root mean square (RMS) value of the controller input voltage value for each axis, $U_x = (\frac{1}{T}\int_0^T |u_x| d_t)^{\frac{1}{2}}$, $U_y = (\frac{1}{T}\int_0^T |u_y| d_t)^{\frac{1}{2}}$, $U_z = (\frac{1}{T}\int_0^T |u_z| d_t)^{\frac{1}{2}}$.

C. Elliptical Contour

A typical 3-D contour, the ellipse, is adapted as desired trajectory which is shown in (39). Fig. 3 gives the desired contour in XYZ plane, and the radius ratio rate is 10 : 1. The unit of contour is meter

$$\begin{cases} x = 0.1(1 - \cos(\omega t)) \\ y = 0.01\sin(\omega t) \\ z = 0.03\sin(\omega t). \end{cases} \tag{39}$$

In the following experiment, let the $\omega = 2rad/s$. For highlighting the robustness of ARC, we mounted a 96 g payload on the experiment platform and additionally add external uncertain disturbance, including a simple coulomb friciton and large step disturbances at control outputs of system block diagram in Simulink artificially. The large step disturbances are three voltage signals lasting three seconds with amplitudes of 0.5, -0.5, 0.5V and coulomb friction disturbances are chosen as $0.2/\pi$

$\arctan(1000\dot{x}), 0.3/\pi \arctan(1000\dot{y}), 0.4/\pi \arctan(1000\dot{z})$ for three axes, where $\dot{x}, \dot{y}, \dot{z}$ are three axes' velocity respectively.

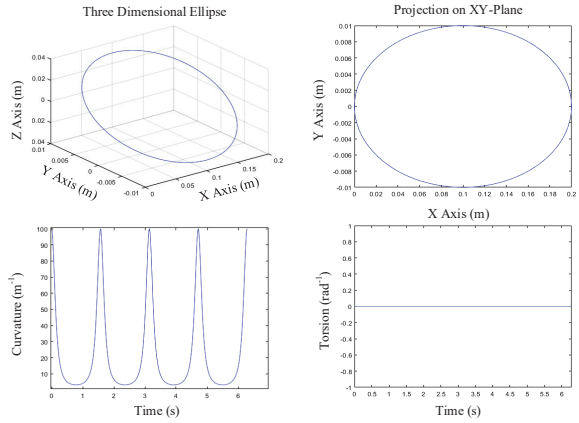

Fig. 3. Desired contour and its curvature

D. Experiment Results

The computed-torque controller (CTC) is set as comparative experiment under system parameters uncertainties and external uncertain disturbance. In following subsections, the CTC parameters which include three parameters are f_t, f_n, f_b all manually adjusted to optimal performance, which are $f_t = 75$Hz, $f_n = 75$Hz, $f_b = 75$Hz.

In ARC, $f(\dot{x})$, $f(\dot{y})$ and $f(\dot{z})$ are respectively chosen as $f(\dot{x}) = 0.2\arctan(1000\dot{x})$, $f(\dot{y}) = 0.3\arctan(1000\dot{y})$, $f(\dot{z}) = 0.5\arctan(1000\dot{z})$. The designed parameter Λ is equal to $\mathrm{diag}[90,90,90]$. By (26) , the robust controller $\mathbf{u_r}$ can be written as $\mathbf{u_r} = -\mathbf{K_s s}$ in the experiment, where $\mathbf{K_s} = \mathrm{diag}[40,60,0]$. The adaption rates Γ are set as $\mathrm{diag}[900,900,900,900,900,900,1000,1000,1000,1000,1000,1000]$. $\hat{\theta}(0) = [0.0261, 0.0268, 0.0265, 24.00, 24.2, 24.10, 0, 0, 0, 0, 0, 0]^{\mathrm{T}}$ which is the initial value of $\hat{\theta}(0)$. The θ_{max} and θ_{min} are chosen as

$$\theta_{min} = [0.0264, 0.0264, 0.0264, 23, 23, 23, 0, 0, 0, -1, -1, -1]^T$$
$$\theta_{max} = [0.0366, 0.0366, 0.0366, 25, 25, 25, 0.2, 0.2, 0.2, 1, 1, 1]^T.$$

The latter experiment results are divided into five groups which are named G0, G1, G2, G3 and G4. G0 has neither load nor artificially external uncertain disturbance. G1 has a 96-g load and no artificially external uncertain disturbance. G2 is only subjected to coulomb friction disturbances and has a 96-g load, G3 is only subjected to large step disturbances and has a 96-g load, and G4 is disturbed by coulomb friction and large step signal and has a 96-g payload simultaneously.

In Table I, the value of evaluation index are given. For G0 and G1, both ARC and CTC achieve better contouring precision in spite of inertia load changed from Table I and Fig. 4. The ARC performs on contour better than CTC, thus the advantages of proposed ARC on system dynamic parameter uncertainties are verified. And maximum value of contouring error of CTC and ARC is in the range of encoder precision which is 0.5 μm.

TABLE I
ELLIPTICAL CONTOURING EXPERIMENT RESULT

	ε_m (μm)	ε_r (μm)	e_r (μm)	U_x (V)	U_y (V)	U_z (V)
CTC(G0)	12.52	1.92	3.20	3.37	0.34	1.03
ARC(G0)	12.43	2.08	2.44	3.41	0.34	1.02
CTC(G1)	12.86	2.32	3.34	3.35	0.34	1.03
ARC(G1)	12.71	2.43	2.66	3.45	0.33	1.00
CTC(G2)	43.31	16.59	23.02	3.42	0.38	1.08
ARC(G2)	51.69	4.94	5.38	3.40	0.38	1.08
CTC(G3)	151.16	67.05	79.14	3.40	0.43	1.06
ARC(G3)	150.23	9.40	11.77	3.42	0.42	1.04
CTC(G4)	159.72	68.95	82.04	3.42	0.47	1.11
ARC(G4)	161.97	10.07	13.27	3.38	0.47	1.12

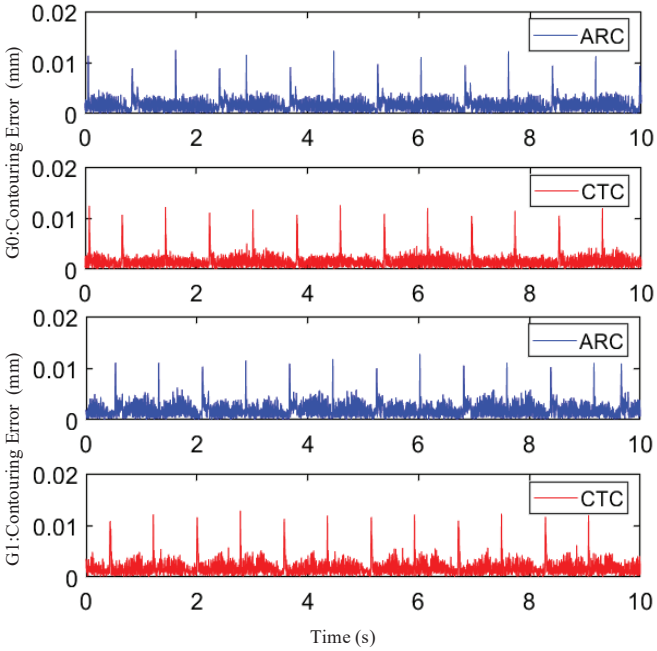

Fig. 4. Contouring errors of G0 and G1

The contouring errors under artificially external uncertain disturbances are given in Fig. 5 and experiment results showed in Table I. The performance of ARC is far superior to CTC on ε_r and e_r. Especially, when the system is disturbed by simple coulomb friction, large step signal and carried with a 96-g payload simultaneously, the RMS value of ε_c and e of ARC method is reduced by 58.88 μm and 68.77 μm, respectively, compared with CTC's, the ε_r has been reduced 70%, 86% and 85%. From the ε_r in Table I, the added simple coulomb friction disturbances and large step disturbance hardly not affect the contouring precision of ARC except the instantaneous spikes when the disturbances suddenly emerge and disappear. All these results show the outstanding performance of the proposed schemes under externally uncertain disturbances.

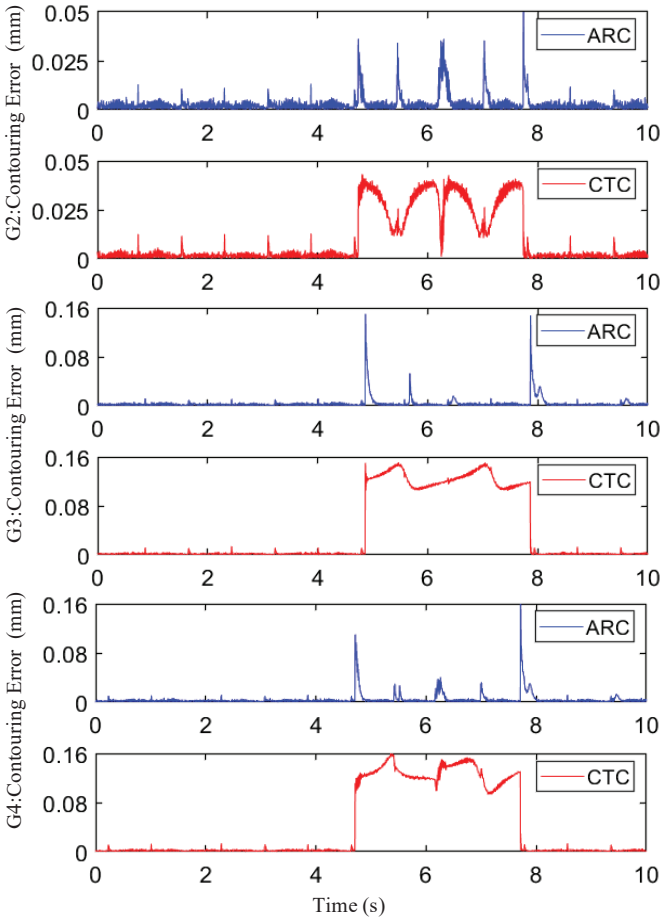

Fig. 5. Contouring errors of G2, G3 and G4

V. Conclusion

For improving contouring precision, under system dynamic parameters uncertainties and externally uncertain disturbances in TCCF, including simple coulomb friction disturbances and large step disturbances, an adaptive robust controller (ARC) is employed in TCCF for a three-axis servo system. Experiment of large curvature ellipse contour shows that the proposed method can get higher overall trajectory performance during externally disturbance occurring and the robustness to variable system model. Compared with CTC, ε_r has been reduced 70%, 86% and 85%, respectively, under simple column friction, step disturbance and all of them in TCCF based on ARC.

References

[1] Zhenyuan Jia, Jianwei Ma, Dening Song, Fuji Wang, and Wei Liu. A review of contouring-error reduction method in multi-axis CNC machining. *International Journal of Machine Tools and Manufacture*, 125:34–35, 2018.

[2] Yoram Koren. Cross-coupled biaxial computer control for manufacturing systems. *Journal of Dynamic Systems, Measurement, and Control*, 102(4):265–272, 1980.

[3] Ran shi, Yunjiang Lou, Xiang Zhang, and Jianggang Li. A Novel Task Coordinate Frame Reduced-Dimension 3-D Contouring Control. *IEEE Transaction on Automation Science and Engineering*, 15(4):1852–1863, 2018.

[4] Bin Yao, Chuxiong Hu, and Qingfeng Wang. An orthogonal global task coordinate frame for contouring control of biaxial systems. *IEEE/ASME Transactions on Mechatronics*, 17(4):622–634, 2012.

[5] G.T.-C. Chiu and Masayoshi Tomizuka. Contouring control of machine tool feed drive systems: a task coordinate frame approach. *IEEE Transactions on Control system and Technology*, 9(1):130–139, 2001.

[6] Yunjiang Lou, Meng Hao, Jiangzhao Yang, Zexiang Li, Jian Gao, and Xin Chen. Task polar coordinate frame-based contouring control of biaxial systems. *IEEE Transactions on Industrial Electronics*, 61(7):3490–3501, 2014.

[7] Bin Yao and Masayoshi Tomizuka. Smooth robust adaptive sliding mode control of robot manipulators with guaranteed transient performance. *Journal of Dynamic Systems, Measurement and Control*, 118(4):764–775, 1996.

[8] Bin Yao. High performance adaptive robust control of nonlinear systems: A general framework and new schemes. In *Proceedings of IEEE Conference on Decision and Control, San Diego*, pages 2489–2494. IEEE, 1997.

[9] Chuxiong Hu, Bin Yao, and Qingfeng Wang. Coordinated adaptive robust contouring controller design for an industrial biaxial precision gantry. *IEEE/ASME Transactions on Mechatronics*, 15(5):728–735, 2010.

[10] Ran shi and Yunjiang Lou. A novel contouring error estimate for three-dimensional contouring control. *IEEE Robotics and Automation Letters*, 2(1):128–134, 2016.

[11] Azad Ghaffari and A. Galip Ulsoy. Dynamic Contour Error Estimation and Feedback Modification for High-Precision Contouring. *IEEE/ASME Transactions on Mechatronics*, 21(3):1732–1741, 2016.

[12] Jian Zhang, Chuxiong Hu, Bin Yao, Qingfeng Wang, and Cong Li. System identification, modeling and precision motion control of a linear motor drive stage. In *Proceedings of 2010 IEEE International Conference on Automation and Logistics, Hong Kong and Macau*, pages 226–231. IEEE, 2010.